

A Polyoxometalate-templated Inorganic-Organic Hybrid Compound Containing a Crown-like Metallamacrocyclic Cation $[\text{Ag}_6(1,2,4\text{-triazole})_6]^{6+}$

Xiang-Min Chen, De-Song Wang, Qing-Zhi Luo, and Ran Wang

Postgraduate Admissions Office, Hebei University of Science and Technology,
Shijiazhuang 050018, P.R. China

Reprint requests to Xiangmin Chen. E-mail: chenxm1995@yahoo.com.cn

Z. Naturforsch. **2008**, 63b, 489–495; received January 2, 2008

A new polyoxometalate(POM)-templated inorganic-organic hybrid compound, $[\text{Ag}_6(\text{trz})_6]^{6+} \cdot [\text{PMo}_{12}\text{O}_{40}]_2 \cdot 6\text{H}_2\text{O}$ (**1**) (trz = 1,2,4-triazole) has been prepared under hydrothermal conditions and characterized by single-crystal X-ray diffraction, elemental analyses, IR spectroscopy, thermogravimetric analysis and cyclic voltammetry. In compound **1**, six Ag^+ ions are linked by six trz molecules to give a hexanuclear $[\text{Ag}_6(\text{trz})_6]^{6+}$ cycle. The six trz molecules are not co-planar, but adopt a crown-like shape. Cavities, with sizes of about $7.706 \times 7.706 \text{ \AA}^2$, are found with the hexanuclear cycles packed along the *c* axis. The Keggin anions, as templates, are inserted in the 3D supramolecular framework. The electrochemical and electrocatalytic behavior of **1** has been studied in detail. The results exhibit that the redox ability of the Keggin anions can be maintained in the hybrid solid which has good electrocatalytic activity toward the reduction of bromate, hydrogen peroxide and nitrite.

Key words: Keggin Anion, Metallamacrocycle, POM-templated Hybrid, Electrochemistry

Introduction

In recent years, the research on new large porous materials, such as zeolites and zeolite-like compounds, has attracted considerable attention because these materials have many potential applications in catalysis, as molecular sieves, in gas separation and as ion exchangers [1–3]. These compounds are typically synthesized under hydrothermal conditions by using organic molecules (such as amines) as templates. However, up to now, there are relatively few reports on the design and synthesis of new porous compounds by using large inorganic anions as templates, in combination with metal ions, organic molecules or metal-organic subunits as host moieties in the assembly process [4, 5]. Polyoxometalates (POMs), as a unique class of metal-oxide clusters, constitute an appealing branch of inorganic systems owing to their structural diversity as well as wide-ranging applications in topology, catalysis, medicine, magnetism, photochemistry, and electrochemistry [6–10]. Therefore POMs are extensively utilized as large inorganic anionic templates to construct cationic polymeric hosts. For example, Keller's group used the spherical phosphotungstate ion as a non-coordinating anionic template for the construction of a novel, three-

dimensional Cu(I) coordination polymer [11]. Liu's group has reported the cationic coordination framework $\{[\text{Ni}(4,4'\text{-bpy})_2]^{2+}\}_n$ templated by a V_{16} cluster [12]. Wang *et al.* have hydrothermally synthesized a new double-Keggin-ion-templated, molybdenum-oxide-based organic-inorganic hybrid compound [13]. Peng's group has reported five novel polyoxoanion-templated architectures based on $[\text{As}_8\text{V}_{14}\text{O}_{42}]^{4-}$ and $[\text{V}_{16}\text{O}_{38}\text{Cl}]^{6-}$ building blocks [14].

In this work, we chose the Keggin anion as a template. Furthermore, we used Ag/trz as a metal-organic combination to construct a cationic framework. The Ag/trz system has several advantages: (i) The Ag^+ ion is a suitable choice to construct metal-organic frameworks due to its coordination diversity and flexibility [15–18]. (ii) The 1,2,4-triazole group, given three N donors, is an integration of the coordination geometry of both imidazoles and pyrazoles providing more potential coordination sites [19–22]. It exhibits strong and typical coordination capacity in acting as a bridging ligand to build metal-organic structures. (iii) The features of the Ag^+ ion and the trz ligand allow assembling cationic host units around POM anions with matching size and shape. Herein, we report a new Keggin-anion-templated inorganic-organic hybrid, $[\text{Ag}_6(\text{trz})_6] \cdot [\text{PMo}_{12}\text{O}_{40}]_2 \cdot 6\text{H}_2\text{O}$ (**1**), synthesized

under hydrothermal conditions. In compound **1**, six Ag^+ ions are linked by six trz molecules into a hexanuclear $[\text{Ag}_6(\text{trz})_6]^{6+}$ metallacycle. The Keggin anions, as templates, are inserted into the cavities of the 3D supramolecular $\{[\text{Ag}_6(\text{trz})_6]^{6+}\}_n$ framework. The electrochemical and electrocatalytic behavior of **1** has been studied in detail.

Results and Discussion

Synthesis

The title compound was synthesized under hydrothermal conditions. Many factors, such as the nature of the initial reactants and their stoichiometry, the pH value and the crystallization temperature, may affect the crystal growth and the structure of the products in hydrothermal techniques. Parallel experiments verified that the pH value of the initial reaction system was the crucial factor for the synthesis of the title compound. At pH values higher than three, compound **1** was not obtained.

Description of the structure

A single-crystal X-ray structure analysis has revealed that compound **1** consists of two non-coordinated $[\text{PMo}_{12}\text{O}_{40}]^{3-}$ anions, a hexanuclear $[\text{Ag}_6(\text{trz})_6]^{6+}$ macrocycle and six water molecules. The $[\text{PMo}_{12}\text{O}_{40}]^{3-}$ anions possess the α -Keggin-type structure without disorder. The tetrahedrally coordinated P atom is surrounded by four oxygen atoms with P–O distances ranging from 1.532(6) to 1.539(3) Å, and O–P–O bond angles in the range of 109.4(1)–109.6(1)°. The Mo–O distances vary over a wide range, 1.673(4)–2.436(3) Å, and can be divided into three groups: (i) The Mo–Od (O_d = terminal oxygen) bonds are in the usual range of 1.673(4)–1.687(4) Å; (ii) Mo–Ob/c ($\text{O}_{b/c}$ = bridging oxygen) distances vary from 1.849(3) to 1.983(3) Å; (iii) the longest Mo–Oa

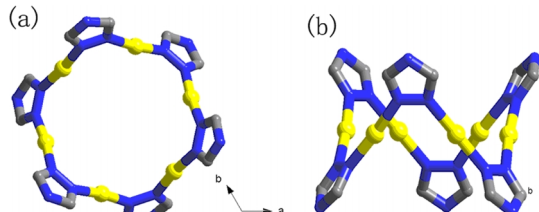


Fig. 1. (a) The hexanuclear $[\text{Ag}_6(\text{trz})_6]^{6+}$ metallamacrocyclic structure viewed along the c axis. (b) The crown-like shape of the cycle along the given direction. Color codes (online): yellow, Ag^+ ion; blue, N atom; gray, C atom.

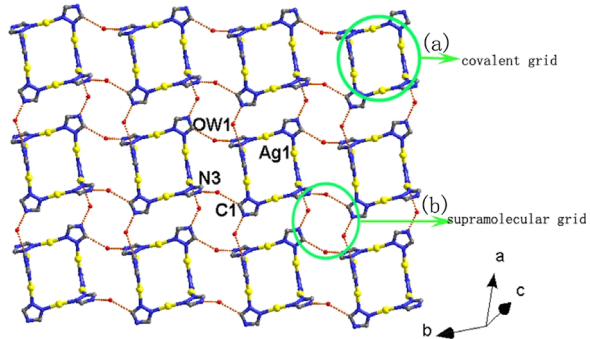


Fig. 2. The grid layer in the crystals of compound **1**. (a) The covalent grid of $[\text{Ag}_6(\text{trz})_6]^{6+}$ cycles. (b) The tetranuclear supramolecular grid formed by hydrogen bonds $\text{OW1}\cdots\text{N3}$ and $\text{OW1}\cdots\text{C1}$.

(O_a = oxygen coordinated with the P atom) bonds are in the range of 2.427(3)–2.436(3) Å. The P–O and Mo–O lengths are in the normal ranges [23].

In a $[\text{Ag}_6(\text{trz})_6]^{6+}$ subunit, six Ag^+ ions are linked by six trz molecules to construct a hexanuclear $[\text{Ag}_6(\text{trz})_6]^{6+}$ metallacycle (Fig. 1a). Each Ag^+ ion adopts a linear coordination geometry, coordinated by two N atoms from two trz molecules with $\text{Ag}-\text{N}$ bonds of 2.128(5) and 2.132(5) Å, and an angle $\text{N}-\text{Ag}-\text{N}$ of 173.9(2)°. The trz ligand donates adjacent N1 and N2 atoms to build the cycle. The N3 atom is non-coordinated but it is an important hydrogen bonding source for the construction of the supramolecular framework. The six trz molecules are not located in a common plane, but form a crown-like shape (Fig. 1b). However, the six Ag^+ ions are almost in one hexagonal plane with $\text{Ag}-\text{Ag}$ distances of 3.853 Å.

The hexanuclear macrocycles $\{[\text{Ag}_6(\text{trz})_6]^{6+}\}_n$ are connected by the water molecules through hydrogen bonding ($\text{OW1}\cdots\text{N3} = 2.727$ Å, $\text{OW1}\cdots\text{C1} = 3.170$ Å) to construct a supramolecular tetranuclear grid layer (Fig. 2). The covalent grid $[\text{Ag}_6(\text{trz})_6]^{6+}$ is linked by four supramolecular grids with center-to-center distances of about 9.334 Å. On the other hand, the tetranuclear supramolecular grid is also connected by four covalent grids. These layers are further linked through hydrogen bonding into a 3D supramolecular framework. Interestingly, cavities with a size of about 7.706×7.706 Å² are formed by the packing of the units along the c axis. Because the diameter of the Keggin anion (about 10.4 Å) is larger than that of the cavity, the anions can not be surrounded completely by the host metallacycle. Therefore, the anions are inserted into the interspace between adjacent

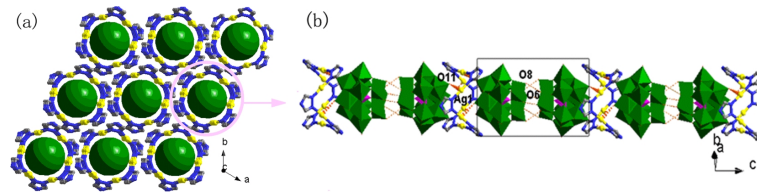


Fig. 3. (a) The Keggin anions inserted into the cavities along the c axis. (b) The dimers of anions inserted between adjacent $[Ag_6(trz)_6]^{6+}$ cycles with a sequence ABAB (inside of the rectangle: anionic dimer).

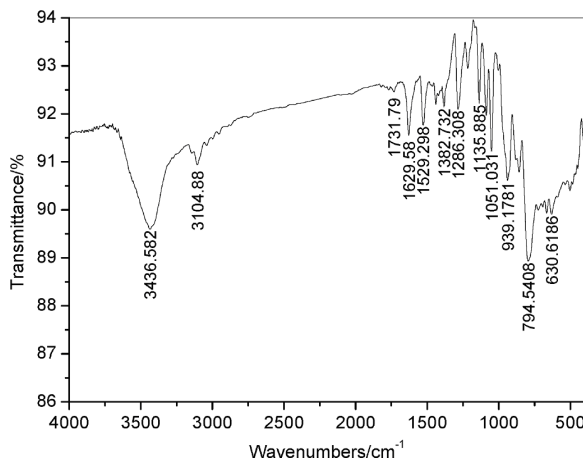


Fig. 4. IR spectrum of compound **1**.

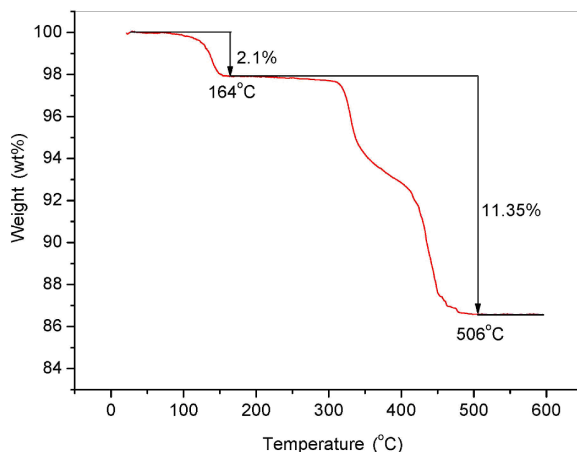


Fig. 5. TG curve of compound **1**.

$[Ag_6(trz)_6]^{6+}$ cycles (Fig. 3a). Two Keggin anions are linked by short interactions of $O_6 \cdots O_8$ (2.931 \AA) to form a supramolecular dimer. The dimer inserts into the vacancy between two adjacent cycles in an ABAB sequence (Fig. 3b).

IR spectrum

The IR spectrum of compound **1** exhibits the characteristic bands of the α -Keggin structure at 939, 848,

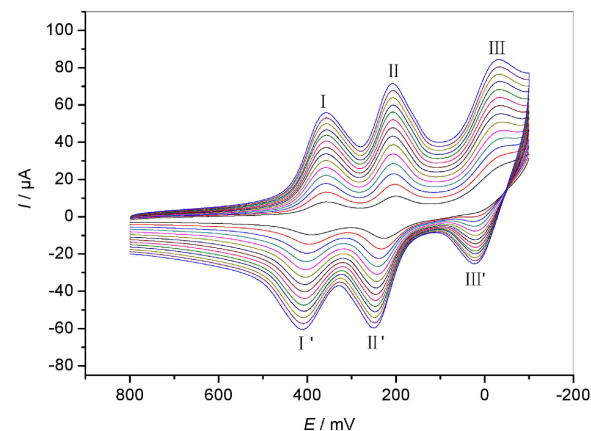


Fig. 6. The cyclic voltammograms of the **1**-CPE in 1 M H_2SO_4 at different scan rates (from inner to outer: 40, 60, 80, 100, 120, 140, 160, 180, 200, 220, 240, 260, 280 and $300 \text{ mV} \cdot \text{s}^{-1}$).

794, and 1051 cm^{-1} attributed to $\nu(Mo-O_t)$, $\nu(Mo-O_b-Mo)$, $\nu(Mo-O_c-Mo)$, and $\nu(P-O)$. The bands at $1135-1731 \text{ cm}^{-1}$ are characteristic of the trz molecules (Fig. 4).

TG analysis

The TG curve of compound **1** is shown in Fig. 5. It exhibits three steps of weight losses. The first weight loss (2.1 %) in the range of 25–164 °C corresponds to the release of the non-coordinated water molecules (calcd. 2.25 %). The last two continuous weight losses (11.35 %) in the range of 205–506 °C correspond to the loss of the trz molecules (calcd. 11.44 %).

Cyclovoltammetry

Voltammetric behavior of **1**-CPE in an aqueous electrolyte

Compound **1** as synthesized under hydrothermal conditions is insoluble in water and common organic solvents. Therefore, the carbon paste electrode (CPE) becomes the optimal choice to study its electrochemical properties. The CPE has some merits: (i) It is inexpensive, easy to prepare and to handle. (ii) It has

long-term stability and allows for surface-renewal by simple mechanical polishing.

Fig. 6 shows the cyclic voltammograms for **1**-CPE in 1 M H₂SO₄ aqueous solution at different scan rates. Three reversible redox peaks appear in the potential range from +800 to -100 mV. The half-wave potentials $E_{1/2} = (E_{pa} + E_{pc})/2$ are +376 (I-I'), +217 (II-II') and -6 (III-III') mV (scan rate: 60 mV·s⁻¹), respectively. Three pairs of redox waves should be attributable to three consecutive two-electron processes of Mo(VI/V) couples, which are usually observed in other PMo₁₂-modified systems [10, 24–26]. The redox wave of the Ag⁺ ion is not detected in the scan range from +800 and -100 mV. This phenomenon was also observed in similar PMo₁₂/Cu systems, for which the redox wave of Cu²⁺/Cu⁺ is absent, such as in (NH₄)[Cu₂₄I₁₀L₁₂][PMo^V₂Mo^{VI}₁₀O₄₀]₃-CPE (L = 4-[3-(1H-1,2,4-triazol-1-yl)propyl]-4H-1,2,4-triazole) [10] and [Cu^I₂(DF)₂H₂O][HPMo^{VI}₁₀Mo^V₂O₄₀{Cu^{II}(DF)}]-CPE (DF = 4,5-diazafluoren-9-one) [27]. The peak potentials change gradually following the scan rates from 40 to 300 mV·s⁻¹: the cathodic peak potentials shift in the negative direction and the corresponding anodic peak potentials in the positive direction with increasing scan rates. The redox ability of the parent α -Keggin anion is maintained in the hybrid solid of **1**.

pH-Dependent electrochemical behavior of **1**-CPE

The acidity of the supporting electrolyte has a remarkable effect on the electrochemical behavior of **1**-

CPE. Fig. 7 shows cyclic voltammograms for **1**-CPE in H₂SO₄ + Na₂SO₄ solutions at various pH values. With increasing pH, the three peak potentials all shift gradually in the negative potential direction, and the peak currents decrease. Reduction of compound **1** in the CPE is accompanied by the evolution of protons from the solution to the wetted electroactive section of the electrode to maintain charge neutrality. Along with increasing pH, slower penetration of protons to the wetting section of the **1**-CPE is probably the reason for the current decrease. The more negative reduction potentials can be elucidated by the Nernst equation. This effect was also observed in Mo₉O₂₆⁻ and P₂Mo₁₈-modified CCEs [28, 29] and a (H_{3/4}pbpy)₄[PMo₁₂O₄₀]-modified CPE [30].

Electrocatalytic reduction of bromate, hydrogen peroxide and nitrite on **1**-CPE

Many studies have shown that Keggin-type POMs can be used as effective electrocatalysts. For example, Zhu's group has reported PMo₁₂-modified CCEs and a GeMo₁₂-modified GOSE, which show high electrocatalytic activities toward the oxidation of ascorbic acid and the reduction of nitrite, bromate and hydrogen peroxide, respectively [31, 32]. Kulesza's group has reported hybrid inorganic-organic films, which are functionalized and exhibit electrocatalytic properties towards reduction of nitrite, bromate and hydrogen peroxide or oxygen [33]. In this work, we found that **1**-CPE also has a good electrocatalytic activity for the reduction of bromate, hydrogen peroxide and nitrite.

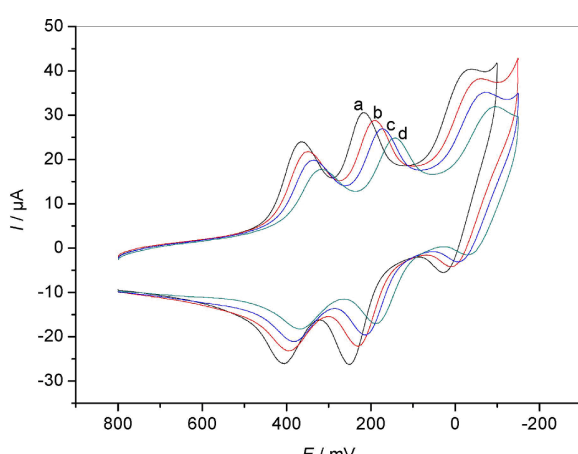


Fig. 7. The cyclic voltammograms of the **1**-CPE in H₂SO₄ + Na₂SO₄ solutions with different pH: (a) 0.7; (b) 1.0; (c) 1.28; (d) 1.64. Scan rate: 100 mV·s⁻¹.

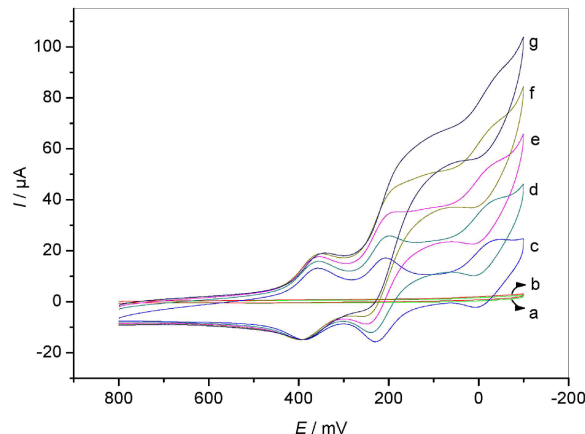


Fig. 8. Cyclic voltammograms of a bare CPE in 1 M H₂SO₄ containing 0 (a) and 12 (b) mM NaBrO₃; **1**-CPE in 1 M H₂SO₄ containing 0 (c); 5 (d); 10 (e); 15 (f); 20 (g) mM NaBrO₃. Scan rate: 100 mV·s⁻¹.

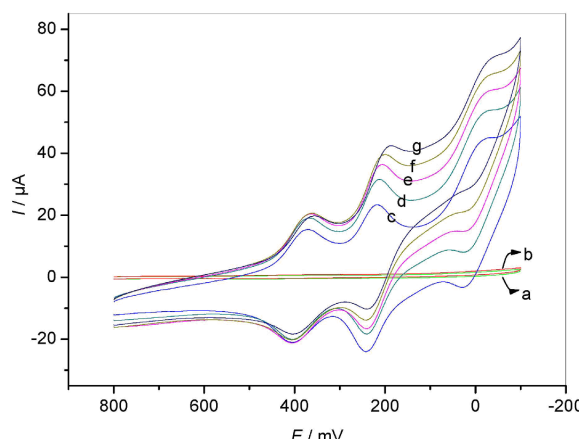


Fig. 9. Cyclic voltammograms of a bare CPE in 1 M H₂SO₄ containing 0 (a) and 16 (b) mM H₂O₂; 1-CPE in 1 M H₂SO₄ containing 0 (c); 4 (d); 8 (e); 16 (f); 32 (g) mM H₂O₂. Scan rate: 100 mV · s⁻¹.

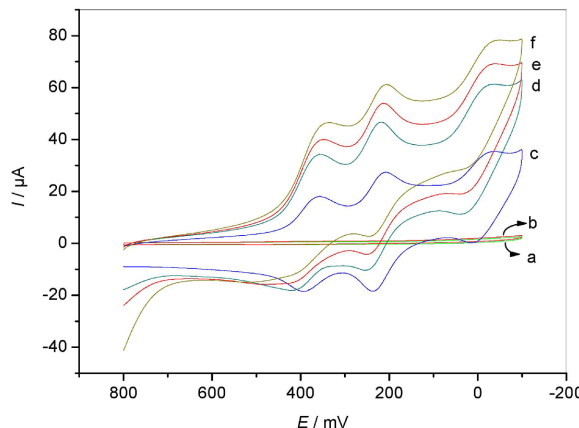


Fig. 10. Cyclic voltammograms of a bare CPE in 1 M H₂SO₄ containing 0 (a) and 16 (b) mM NaNO₂; 1-CPE in 1 M H₂SO₄ containing 0 (c); 4 (d); 8 (e); 16 (f) mM NaNO₂. Scan rate: 100 mV · s⁻¹.

Fig. 8 shows cyclovoltammograms for the electrocatalytic reduction of bromate at a bare CPE and at 1-CPE in 1 M H₂SO₄ aqueous solution. No obvious voltammetric response is observed at a bare CPE in 1 M H₂SO₄ aqueous solution containing 12 mM bromate in the potential range from +800 to -100 mV. At the 1-CPE, with the addition of bromate, the second and the third reduction peak currents increase gradually while the corresponding oxidation peak currents gradually decrease. However, the first redox peak remains almost unchanged, which indicates that the four- and six-electron reduced species of the PMo₁₂ anions have electrocatalytic activity at

1-CPE for the reduction of bromate. Furthermore, it has been noted that the six-electron-reduction species has the highest catalytic activity toward the reduction of bromate. Fig. 9 shows a similar electrocatalytic behavior for the reduction of hydrogen peroxide. It indicates that the four- and six-electron reduced species of PMo₁₂ anions also show electrocatalytic activity at 1-CPE for the reduction of hydrogen peroxide.

Fig. 10 shows the electrocatalytic reduction of nitrite by 1-CPE in 1 M H₂SO₄ aqueous solution. The behavior is different from the reduction of bromate and hydrogen peroxide. All three reduction peak currents gradually increase while the corresponding oxidation peak currents decrease, suggesting that nitrite is reduced by two-, four- and six-electron reduced species of PMo₁₂ anions.

Conclusions

In this work, a new POM-templated inorganic–organic hybrid compound has been synthesized under hydrothermal conditions. In compound **1**, six Ag⁺ ions are linked by six trz molecules to give a hexanuclear [Ag₆(trz)₆]⁶⁺ macrocycle. The cavities, formed in the packing of these cycles along the *c* axis, are occupied by the Keggin anions. The anion dimers are inserted into the vacancies between adjacent metallacycles. A 3D supramolecular framework is built by hydrogen bonding. Given the variations in the polyoxometalate clusters and the diversity of the metal–organic moieties, the scope for further syntheses of POM-templated compounds appears to be great.

Experimental Section

Materials and methods

All reagents were of reagent grade and were used as received from commercial sources without further purification. Elemental analyses (C, H and N) were performed on a Perkin-Elmer 2400 CHN elemental analyzer. The IR spectrum was obtained on an Alpha Centaur FT/IR spectrometer with a KBr pellet in the region 400–4000 cm⁻¹. The thermogravimetric analysis (TGA) was carried out in N₂ on a Perkin-Elmer DTA 1700 differential thermal analyzer with a rate of 10.00 °C min⁻¹. Electrochemical measurements were performed with a CHI 660b electrochemical workstation. A conventional three-electrode system was used. The working electrode was a modified carbon paste electrode (CPE). An Ag/AgCl (3 M KCl) electrode was used as a reference electrode and a Pt wire as a counterelectrode.

Table 1. Crystal structure data for compound **1**.

Formula	$C_{12}H_{24}Ag_6Mo_{24}N_{18}O_{86}P_2$
M_f	4808.12
Crystal system	rhombohedral
Space group	$R\bar{3}$
$a, \text{\AA}$	18.0806(6)
$c, \text{\AA}$	23.2138(10)
$V, \text{\AA}^3$	6572.1(4)
Z	3
T, K	273(2)
$D_{\text{calcd}}, \text{g cm}^{-3}$	3.64
$\mu(\text{Mo}K\alpha), \text{cm}^{-1}$	47.78
$F(000), e$	6654
hkl range	$-24 \rightarrow +18, -20 \rightarrow +24,$ $-29 \rightarrow +30$
$((\sin \theta)/\lambda)_{\text{max}}, \text{\AA}^{-1}$	0.667
Absorption correction; T_{\min}/T_{\max}	numerical; 0.30/0.68
Refl. measured	13605
Refl. unique	3637
R_{int}	0.032
Param. refined	223
$R(F)/wR(F^2)^a [I \geq 2\sigma(I)]$	0.031/0.078
$R(F)/wR(F^2)^a$ (all data)	0.040/0.083
$GOF(F^2)$	1.032
$\Delta\rho_{\text{fin}} (\text{max/min}), e \text{\AA}^{-3}$	1.79/−1.35

^a $R_1 = \sum \|F_o\| - |F_c\| / \sum |F_o\|$; $wR_2 = \left[\sum [w(F_o^2 - F_c^2)^2] / \sum [w(F_o^2)^2] \right]^{1/2}$; $w = 1/[\sigma^2(F_o^2) + (0.0392P)^2 + 54.3096P]$ where $P = (F_o^2 + 2F_c^2)/3$.

Synthesis

[Ag₆(trz)₆][PMo₁₂O₄₀]₂·6H₂O (**1**)

A mixture of H₃[PMo₁₂O₄₀]·xH₂O (0.22 g, 0.045 mmol), AgNO₃ (0.085 g, 0.5 mmol) and trz (0.021 g, 0.3 mmol) was dissolved and suspended in 10 mL of distilled water at r.t. After the pH value of the mixture was adjusted to about 2.6 with 1.0 M NaOH, the suspension was put into a Teflon-lined autoclave and kept under autogenous pressure at 160 °C for 4 days. After slow cooling to r.t., yellow block-shaped crystals were filtered and washed with distilled water (40% yield based on Mo). C₁₂H₂₄Ag₆Mo₂₄N₁₈O₈₆P₂ (4808.12): calcd. C 2.99, H 0.5, N 5.24; found C 2.92, H 0.47, N 5.18.

X-Ray crystallography

A yellow single crystal of **1** with dimensions 0.28 × 0.22 × 0.08 mm³ was glued on a glass fiber. Data were collected on a CCD diffractometer with graphite-monochromated MoK α radiation ($\lambda = 0.71073 \text{\AA}$) at 273 K. The structure was refined by the full-matrix least-squares method on F^2 using the SHELX crystallographic software package [34].

Table 2. Selected bond lengths (Å) and bond angles (deg) for compound **1**^a.

P(1)–O(1)	1.532(6)	Mo(3)–O(10)	1.861(3)
P(1)–O(2)	1.539(3)	Mo(3)–O(6)	1.976(4)
P(1)–O(2) ^{#1}	1.539(3)	Mo(3)–O(13)	1.983(3)
P(1)–O(2) ^{#2}	1.539(3)	Mo(3)–O(1)	2.436(3)
Mo(1)–O(4)	1.675(4)	Mo(4)–O(11)	1.687(4)
Mo(1)–O(13)	1.856(3)	Mo(4)–O(12) ^{#2}	1.849(3)
Mo(1)–O(14) ^{#2}	1.922(3)	Mo(4)–O(7)	1.872(4)
Mo(1)–O(9)	1.924(3)	Mo(4)–O(5)	1.970(4)
Mo(1)–O(7)	1.970(4)	Mo(4)–O(12)	1.974(3)
Mo(1)–O(2)	2.429(3)	Mo(4)–O(2)	2.428(3)
Mo(2)–O(3)	1.682(4)	O(1)–Mo(3) ^{#1}	2.436(3)
Mo(2)–O(5)	1.872(4)	O(1)–Mo(3) ^{#2}	2.436(3)
Mo(2)–O(14)	1.899(3)	O(6)–Mo(3) ^{#1}	1.861(3)
Mo(2)–O(9)	1.931(3)	O(10)–Mo(2) ^{#2}	1.947(3)
Mo(2)–O(10) ^{#1}	1.947(3)	O(12)–Mo(4) ^{#1}	1.849(3)
Mo(2)–O(2)	2.427(3)	O(14)–Mo(1) ^{#1}	1.922(3)
Mo(3)–O(8)	1.673(4)	Ag(1)–N(1)	2.128(5)
Mo(3)–O(6) ^{#2}	1.861(3)	Ag(1)–N(2)	2.132(5)
N(1)–Ag(1)–N(2)	173.9(2)	C(2)–N(1)–Ag(1)	126.3(4)

^a Symmetry codes: ^{#1} $-x + y, -x + 1, z$; ^{#2} $-y + 1, -x - y + 1, z$.

Anisotropic thermal parameters were used to refine all non-hydrogen atoms. All the hydrogen atoms attached to carbon atoms were generated geometrically, while the hydrogen atoms attached to water molecules were not located. The crystal and structure refinement data for compound **1** are summarized in Table 1. Selected bond lengths (Å) and angles (deg) are listed in Table 2.

CCDC 670662 contains the supplementary crystallographic data for this paper. These data can be obtained free of charge from The Cambridge Crystallographic Data Centre via www.ccdc.cam.ac.uk/data_request/cif.

Preparation of **I**-CPE

The compound **1**-modified CPE (**1**-CPE) was fabricated as follows: 75 mg of graphite powder and 6 mg of **1** were mixed and ground together using an agate mortar and pestle to achieve a uniform mixture, and then 0.1 mL of Nujol was added with stirring. The homogenized mixture was packed into a glass tube with a 1.5 mm inner diameter, and the tube surface was wiped with paper. The electrical contact was established with a copper rod through the back of the electrode.

Acknowledgement

This work was financially supported by the Doctoral Research Fund for Hebei Higher Learning Institutions (05547004D-1).

- [1] G. M. Wang, J. Y. Li, J. H. Yu, P. Chen, Q. H. Pan, H. W. Song, R. R. Xu, *Chem. Mater.* **2006**, *18*, 5637–5639.
- [2] M. Zhang, D. Zhou, J. Y. Li, J. H. Yu, J. Xu, F. Deng, G. H. Li, R. R. Xu, *Inorg. Chem.* **2007**, *46*, 136–140.
- [3] C. H. Lin, S. L. Wang, K. H. Lii, *J. Am. Chem. Soc.* **2001**, *123*, 4649–4650.
- [4] Y. Ishii, Y. Takenaka, K. Konishi, *Angew. Chem.* **2004**, *116*, 2756–2759; *Angew. Chem. Int. Ed.* **2004**, *43*, 2702–2705.
- [5] X. J. Kong, Y. P. Ren, P. Q. Zheng, Y. X. Long, L. S. Long, R. B. Huang, L. S. Zheng, *Inorg. Chem.* **2006**, *45*, 10702–10711.
- [6] D. L. Long, E. Burkholder, L. Cronin, *Chem. Soc. Rev.* **2007**, *36*, 105–121.
- [7] B. Botar, P. Kögerler, C. L. Hill, *Inorg. Chem.* **2007**, *46*, 5398–5403.
- [8] M. L. Wei, C. He, W. J. Hua, C. Y. Duan, S. H. Li, Q. J. Meng, *J. Am. Chem. Soc.* **2006**, *128*, 13318–13319.
- [9] J. A. Fernández, X. López, C. Bo, C. Graaf, E. J. Baerends, J. M. Poble, *J. Am. Chem. Soc.* **2007**, *129*, 12244–12253.
- [10] X. L. Wang, C. Qin, E. B. Wang, Z. M. Su, Y. G. Li, L. Xu, *Angew. Chem.* **2006**, *118*, 7571–7574; *Angew. Chem. Int. Ed.* **2006**, *45*, 7411–7414.
- [11] C. Inman, J. M. Knaust, S. W. Keller, *Chem. Commun.* **2002**, 156–157.
- [12] S. X. Liu, L. H. Xie, B. Gao, C. D. Zhang, C. Y. Sun, D. H. Li, Z. M. Su, *Chem. Commun.* **2005**, 5023–5025.
- [13] Y. G. Li, L. M. Dai, Y. H. Wang, X. L. Wang, E. B. Wang, Z. M. Su, L. Xu, *Chem. Commun.* **2007**, 2593–2595.
- [14] B. X. Dong, J. Peng, C. L. Gómez-García, S. Benmansour, H. Q. Jia, N. H. Hu, *Inorg. Chem.* **2007**, *46*, 5933–5941.
- [15] H. Y. An, Y. G. Li, E. B. Wang, D. R. Xiao, C. Y. Sun, L. Xu, *Inorg. Chem.* **2005**, *44*, 6062–6070.
- [16] Z. G. Han, Y. L. Zhao, J. Peng, H. Y. Ma, Q. Liu, E. B. Wang, N. H. Hu, H. Q. Jia, *Eur. J. Inorg. Chem.* **2005**, *2*, 264–271.
- [17] Q. G. Zhai, X. Y. Wu, S. M. Chen, Z. G. Zhao, C. Z. Lu, *Inorg. Chem.* **2007**, *46*, 5046–5058.
- [18] C. Streb, C. Rirchie, D. L. Long, P. Kögerler, L. Cronin, *Angew. Chem.* **2007**, *119*, 7723–7726; *Angew. Chem. Int. Ed.* **2007**, *46*, 7579–7582.
- [19] J. G. Haasnoot, *Coord. Chem. Rev.* **2000**, 200–202, 131–185.
- [20] X. L. Wang, C. Qin, E. B. Wang, Z. M. Su, *Chem. Commun.* **2007**, 4245–4247.
- [21] Q. G. Zhai, C. Z. Lu, X. Y. Wu, S. R. Batten, *Cryst. Growth Des.* **2007**, *7*, 2332–2342.
- [22] Q. G. Zhai, X. Y. Wu, S. M. Chen, C. Z. Lu, W. B. Yang, *Cryst. Growth Des.* **2006**, *6*, 2126–2635.
- [23] Y. P. Ren, X. J. Kong, X. Y. Hu, M. Sun, L. S. Long, R. B. Huang, L. S. Zheng, *Inorg. Chem.* **2006**, *45*, 4016–4023.
- [24] M. Sadakane, E. Steckhan, *Chem. Rev.* **1998**, *98*, 219–237.
- [25] B. Wang, R. N. Vyas, S. Shaik, *Langmuir*, **2007**, *23*, 11120–11126.
- [26] L. Cheng, J. A. Cox, *Electrochim. Commun.* **2001**, *3*, 285–289.
- [27] A. X. Tian, Z. G. Han, J. Peng, J. Ying, J. Q. Sha, B. X. Dong, J. L. Zhai, H. S. Liu, *Inorg. Chim. Acta*, in press.
- [28] P. Wang, X. P. Wang, G. Y. Zhu, *Electrochim. Acta* **2000**, *46*, 637–641.
- [29] P. Wang, X. P. Wang, Y. Yuan, G. Y. Zhu, *J. Non-Cryst. Solids* **2000**, *277*, 22–29.
- [30] Z. G. Han, Y. L. Zhao, J. Peng, A. X. Tian, Y. H. Feng, Q. Liu, *J. Solid State Chem.* **2005**, *178*, 1386–1394.
- [31] P. Wang, X. P. Wang, X. Y. Jing, G. Y. Zhu, *Anal. Chim. Acta* **2000**, *424*, 51–56.
- [32] P. Wang, Y. Yuan, Z. B. Han, G. Y. Zhu, *J. Mater. Chem.* **2001**, *11*, 549–553.
- [33] K. Karnickaa, M. Chojaka, K. Miecznikowskia, M. Skunika, B. Baranowskaa, A. Kolarza, A. Piranskaa, B. Palysa, L. Adamczykb, P. J. Kuleszaa, *Biochem.* **2005**, *66*, 79–87.
- [34] a) G. M. Sheldrick, *SHELXS-97*, Program for the Solution of Crystal Structures, University of Göttingen, Göttingen (Germany) **1997**; b) G. M. Sheldrick, *SHELXL-97*, Program for the Refinement of Crystal Structures, University of Göttingen, Göttingen (Germany) **1997**.